Young Jun Yang
Sun Hong Kwon
Seung Geun Park
Jun Soo Park

REMOTE SENSING OF WAVE DIRECTIONALITY BY TWO-DIMENSIONAL DIRECTIONAL WAVELETS: PART 1. THE DETECTION TOOLS OF DIRECTIONALITY IN SIGNALS

Summary

This paper presents the results of a study investigating methods of wave directionality based on wavelet transform. In part 1 of this paper, the theoretical background and characteristics of directional wavelet were discussed. Morlet wavelet and Cauchy wavelet were examined to test their efficiency in detection of directionality in signals. These wavelets were tested on numerical images which were considered to describe the basic characteristics of directionality of ocean waves.

Key words: directionality; directional wavelets; morlet wavelet; cauchy wavelet; signal

1. Introduction

The importance of understanding wave directionality has long been recognized in the field of ocean-related science and engineering. It could be a life and death issue to some ship operators. For example, a ship operating in the following sea could lead to dangerous situation by Paulling (1975) [1] and Renilson (1981) [2].The present authors try to propose a scheme which can detect directionality by utilizing directional wavelets by making use of video images of waves. To find out the directionality of ocean waves, the necessary data is just one frame of video images for the proposed scheme. This simplicity in the input data is possible by making use of a directional wavelet. The directional wavelet can be constructed by introducing rotation to one of the continuous wavelets. The introduction of rotation makes it possible to detect edges and directions in the images to be analyzed. The two-dimensional directional wavelet was fully studied by Antoine and Murenzi (1996) [3]. The idea of detection of directionality in signals by using directional wavelet has been studied by wavelet researchers, Antoine et al.(1999) [4], and Antoine and Murenzi (1996) [3,5]. They illustrated the usefulness of angular representation of the continuous wavelet transform (CWT) on the problem of disentangling a train of damped plane waves.

Use was made of directional wavelet to visualize the two dimensional turbulent flow around the obstacle by Wisnoe et al. (1993) [6]. The research on texture orientation was done

by directional wavelet by Rao and Schunck et. al. (1991) [7]. Multi-directional wavelet was proposed by simply superposing the directional wavelet by Watson and Ahumada (1989) [8].

Present study adopted the Morlet wavelet and Cauchy wavelet as directional wavelets. The Morlet wavelet was fully examined to see its usefulness in detection of directional features [3]. It was demonstrated that Cauchy wavelet has excellent angular selectivity. The preset paper is organized as follows. The explanation about the CWT will be given in chapter 2. The description about the directional wavelet will be followed by the theoretical explanation on Morlet and Cauchy wavelet. Then, these wavelets will be tested on the numerical images which are intended to show some characteristics of water waves. Finally, conclusion will be drawn. The applications of the Morlet wavelet and Cauchy wavelet to the more complicated numerical data, wave images taken from small wave flume, river wave images, and ocean wave images will be presented in Part 2 of this paper.

2. Continuous wavelet transforms

The wavelet transform has been successfully applied to many fields, especially in signal and image processing by Meyer (1991) [9], Grossman (1985) [10], and Mallat (1989) [11]. Let's begin with the one-dimensional case of the CWT. The CWT of a signal $s(t)$ is given by

$$W_s(a,b) = \frac{1}{\sqrt{|a|}} \int_{-\infty}^{\infty} \psi^*\left(\frac{t-b}{a}\right) s(t) dt, \tag{1}$$

Where ψ is the wavelet function, a is the scaling parameter, and b is the transform parameter, $*$ represents a complex conjugate. It can be stated that the CWT is the sum over all time of real signal $s(t)$ multiplied by the scaled, shifted wavelet function. The parameter a and b vary continuously in the case of CWT.

A one-dimensional CWT can be easily expanded to a two-dimensional CWT. Its formulation is given by

$$W_s(a,\mathbf{b}) = a^{-1} \int \psi^*(a^{-1}(\mathbf{x}-\mathbf{b})) s(\mathbf{x}) d\mathbf{x}, \tag{2}$$

where $\mathbf{b}$ is the translation parameter and $a>0$ is the dilation parameter. The bold-faced letters represent vectors in this paper. Assume that $s(\mathbf{x})$ is a square integrable function, i.e.,

$$\|s\|^2 = \int |s(\mathbf{x})| d\mathbf{x} < \infty, \tag{3}$$

where $\|\ \|$ denotes the norm. $s(\mathbf{x})$ usually represents the grey level of each pixel in image to be processed. The results of a two-dimensional CWT are a function of three parameters, while the input is two-dimensional. This makes the analysis versatile.

3. Directional Wavelets

Rotation is introduced to detect directionality in the signal, as shown below

$$W_s(a,\theta,\mathbf{b}) = a^{-1} \int \psi^*(a^{-1} r_{-\theta}(\mathbf{x}-\mathbf{b})) s(\mathbf{x}) d\mathbf{x}, \tag{4}$$

where $r_{-\theta} = (x\cos\theta - y\sin\theta, x\sin\theta + y\cos\theta)$ at $0 \leq \theta < 2\pi$.

Remote Sensing of Wave Directionality
by Two-dimensional Directional Wavelets : Part 1.

Young Jun Yang, Sun Hong Kwon
Seung Geun Park, Jun Soo Park

By introducing the rotation parameter, the wavelet function now has translation, rotation, and dilation.

We can see that the right hand side of equation (4) is now a function of direction in addition to the translation and dilation. Directionality can be introduced on the continuous wavelets like Morlet wavelet, multidirectional wavelet, and Cauchy wavelet [3]. The directional characteristics of Morlet wavelet and Cauchy wavelet will be described and tested later in this paper to see which one is an efficient tool in detecting the directionality of signals.

The wavelet transform in the wave number domain with the rotation is written as follows

$$W_s(a, \theta, \mathbf{b}) = a \int e^{i\mathbf{b} \cdot \mathbf{k}} \, \hat{\psi}^*(r_{-\theta}(\mathbf{k})) \, \hat{s}(\mathbf{k}) d\mathbf{k} . \tag{5}$$

The definition of $r_{-\theta}$ can be found below the equation (4). In the light of Parseval's theorem, the wavelet transform can also be done in the frequency domain.

3.1 Morlet wavelet

The formulation of Morlet wavelet can be written as

$$\psi(t) = \pi^{-\frac{1}{4}} (e^{-i\omega_0 t} - e^{-\varpi_0^2/2}) e^{-\frac{t^2}{2}} . \tag{6}$$
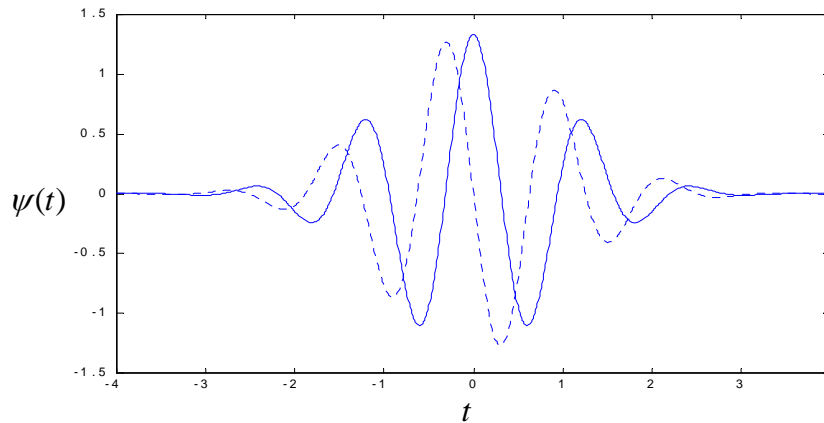
The seconded term is added to satisfy the so-called admissibility condition. However, for large values of ω_0 the correction term is numerically negligible. Thus, the Morlet wavelet can be approximated by the following

$$\psi(t) = \pi^{-\frac{1}{4}} e^{-i\omega_0 t} e^{-\frac{t^2}{2}} . \tag{7}$$

A Fourier transform of the above wavelet is of the following form

$$\hat{\psi}(\varpi) = \pi^{-\frac{1}{4}} e^{-\frac{(\omega - \omega_0)^2}{2}} , \tag{8}$$

where $\hat{\psi}(\varpi)$ represents the Fourier transform of $\psi(t)$.
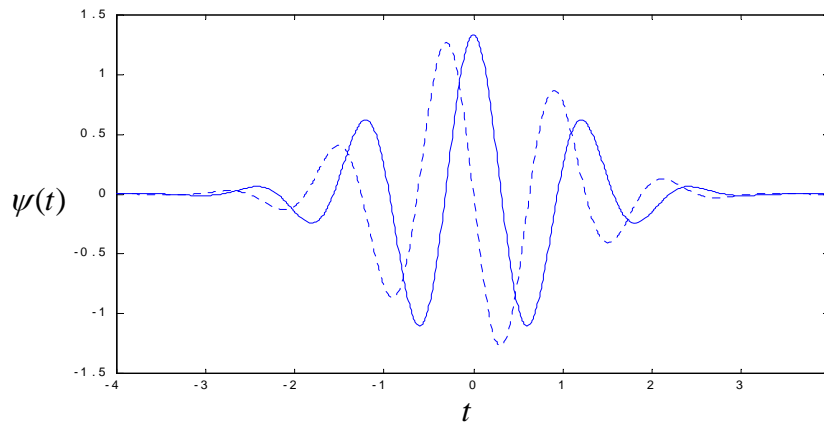

Fig. 1 Real and imaginary part of $\psi(t)$

Fig. 2 Fourier transform of $\psi(t)$

Figure 1 shows the real and imaginary parts of the Morlet wavelet. Its Fourier transform is shown in figure 2. Figure 2 show that the frequency domain is quite confined to a certain range. This property can be useful when we evaluate the wavelet transform because the integral range can be easily determined. This property was utilized in all the computations in this paper.

Let's examine the influence of rotation by using the Morlet wavelet without the correction term, as follows,

$$\psi(\mathbf{x}) = e^{i\mathbf{k}_0 \cdot \mathbf{x}} e^{-\frac{1}{2}(\varepsilon^{-1}x^2 + y^2)} , \tag{9}$$

where $\mathbf{k}_0$ is a wave number vector [rad/m, rad/m] and $\varepsilon > 1$ is an anisotropy parameter. Let's try to examine how these parameters affect the shape of the Morlet wavelet. The first example was done for $\mathbf{k}_0 = (0,5.6)$, $\varepsilon = 1$, and $\theta = 0°$.

Fig. 3 Morlet wavelet : $\mathbf{k}_0 = (0,5.6), \varepsilon = 1, \theta = 0°$.

4

Remote Sensing of Wave Directionality
by Two-dimensional Directional Wavelets : Part 1.

Young Jun Yang, Sun Hong Kwon
Seung Geun Park, Jun Soo Park
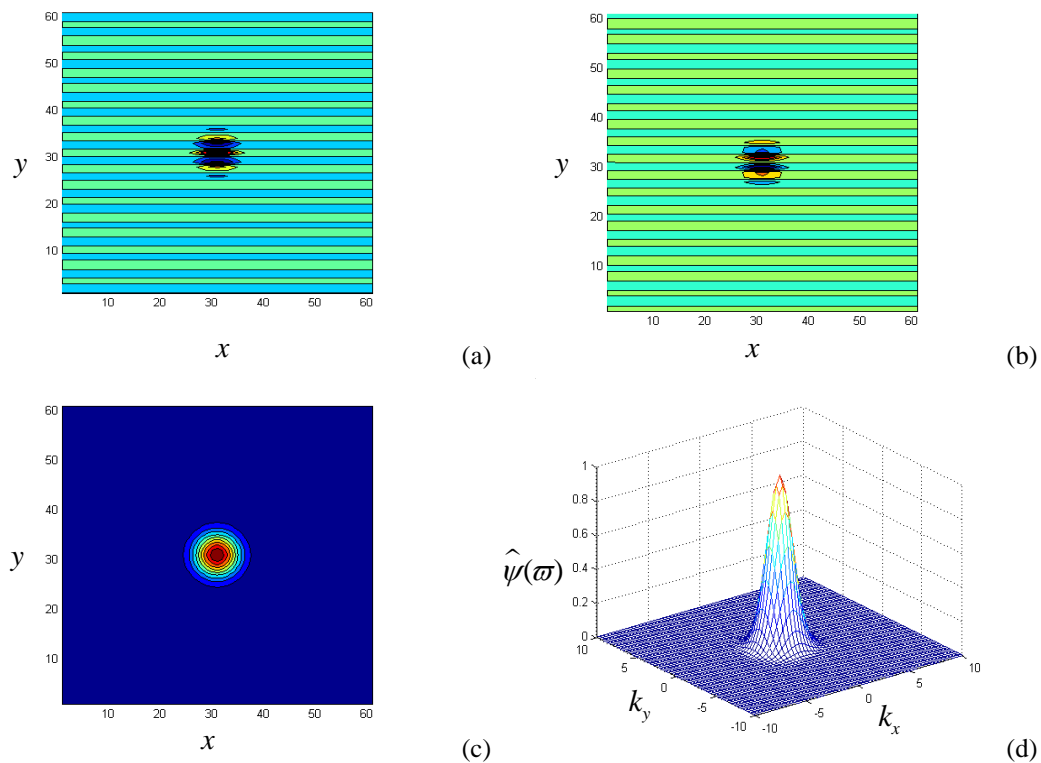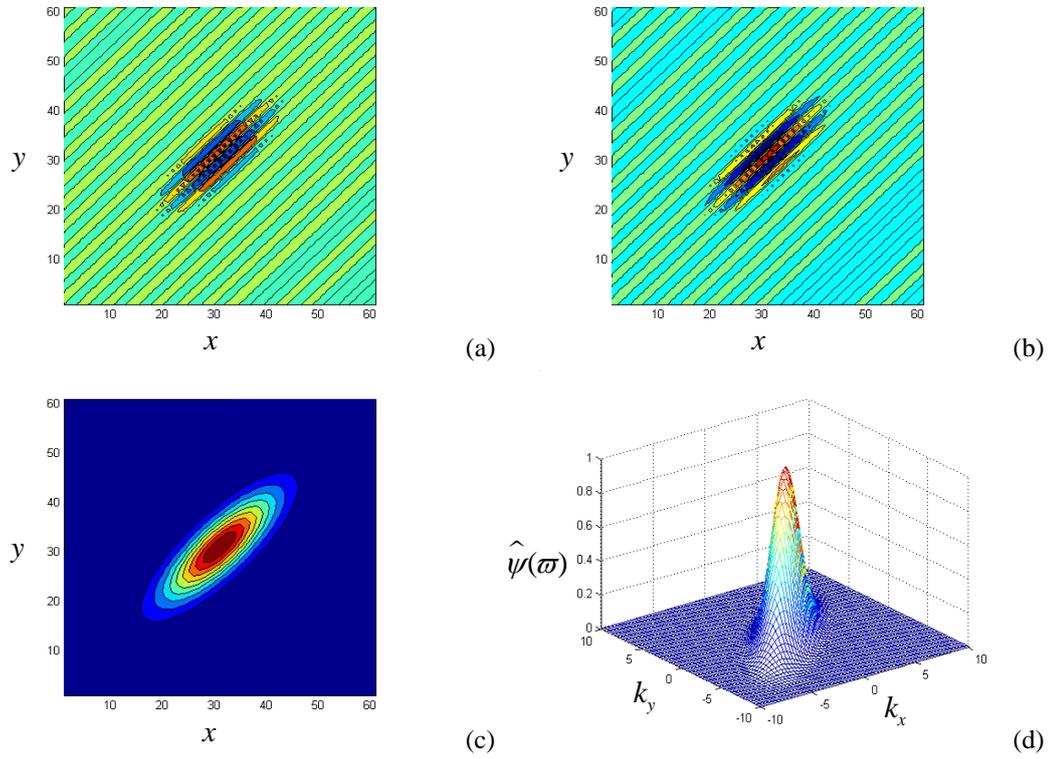
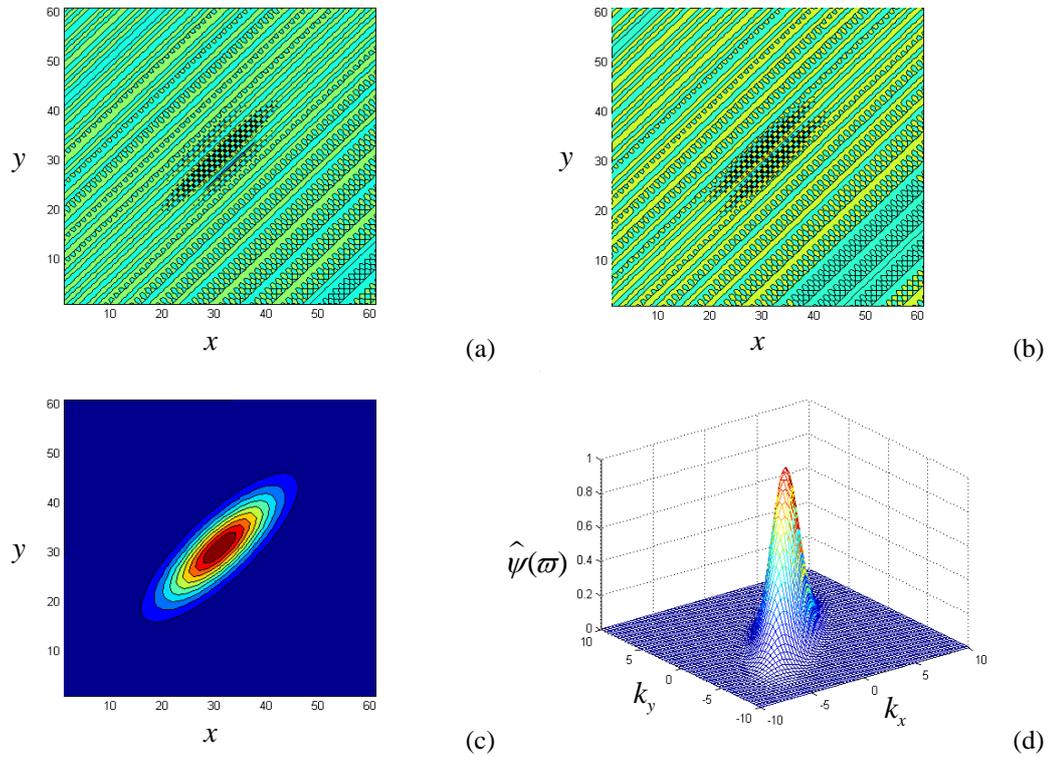**Fig. 4** Morlet wavelet : $\mathbf{k}_0 = (0, 5.6), \varepsilon = 10, \theta = 45°$.

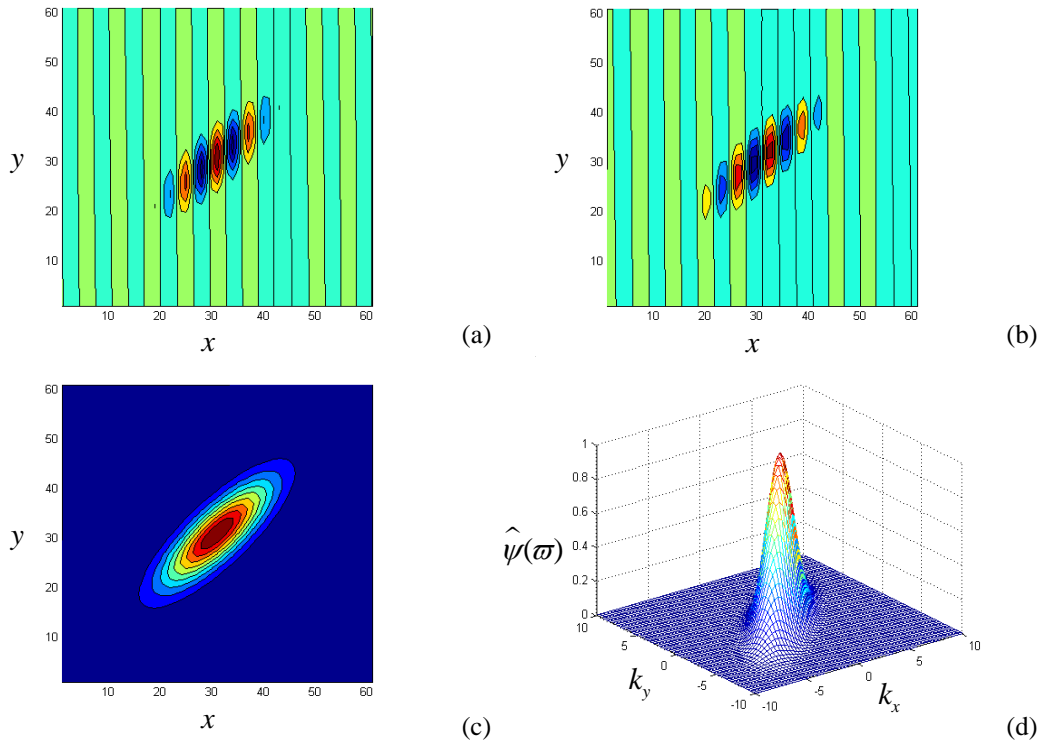**Fig. 5** Morlet wavelet : $\mathbf{k}_0 = (0, 11.2), \varepsilon = 10, \theta = 45°$.

Fig. 6 Morlet wavelet : $\mathbf{k}_0 = (11.2, 11.2), \varepsilon = 10, \theta = 45°$.

The real and imaginary parts of the transformation are shown in figures 3(a) and 3(b). The phase and magnitude in 3-dimensional plot are shown in figures 3(c) and 3(d). Since $\varepsilon = 1$, the base of the convex cone is circle. For $\mathbf{k} = (0, 5.6)$, $\varepsilon = 10$, and $\theta = 45°$ values, the results are presented in figure 4. It can be seen that the effective base of the Gaussian amplitude is changed from circular form to elliptic shape as ε increases. The base now became narrowed. The base of the wavelet has been directed in $45°$. Let's double the y-component of the wave number, i.e., $\mathbf{k} = (0, 11.2)$. The results are shown in figure 5. Since wave number is doubled, the wave length in the signal is reduced by half. Thus, by increasing the magnitude of the wave number, one can achieve a finer angular resolution.

The plot for $\mathbf{k} = (11.2, 11.2)$, $\varepsilon = 10$, and $\theta = 45°$ is shown in figure 6. The wave form for $\theta = 45°$ is rotated again by $45°$ due to the orientation in the wave number, which yields a $90°$ total phase. However, the Gaussian amplitude still remains at $\theta = 45°$. Thus we can select $\mathbf{k} = (0, k_0)$ since taking only the y-component does not result in the loss of its main directional characteristics. Reducing one parameter greatly facilitates the analysis. The expression for $\psi(\mathbf{x})$ without the x-component of the wave number which is used in the present study is given by

$$\psi(\mathbf{x}) = e^{ik_0 y} e^{-\frac{1}{2}(\varepsilon^{-1}x^2 + y^2)} . \tag{10}$$

What we have seen in the above can be verified in the wave number domain as follows. The Fourier transform of the Morlet wavelet is

$$\hat{\psi}(\varpi) = \sqrt{\varepsilon} \exp(-\frac{1}{2}(\varepsilon k_x^2 + (k_y - k_0)^2)) . \tag{11}$$

Remote Sensing of Wave Directionality
by Two-dimensional Directional Wavelets : Part 1.

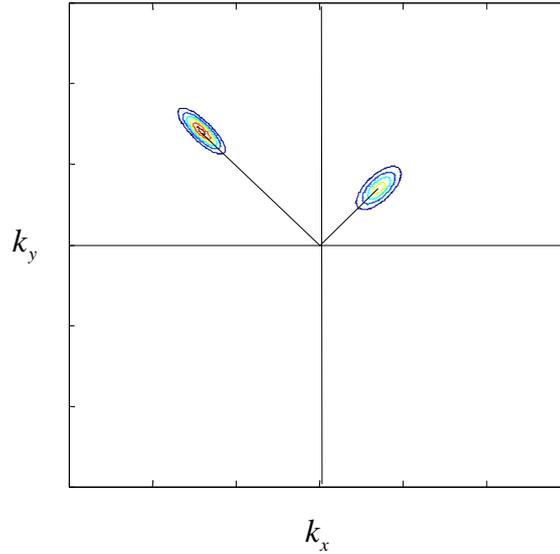Young Jun Yang, Sun Hong Kwon
Seung Geun Park, Jun Soo Park

Fig. 7 Fourier transform of 2-D Morlet wavelet.

Its shape is shown in figure 7 in solid line when ε and k_0 are taken to be 5.6 and it is rotated by 45°. Another line presented in the same figure is the case when $k_0 = 11.2$ and $\varepsilon = 10$, and rotated by 135°. As can be seen from figure 7, the base of the convex cone becomes narrow when ε increases. By increasing the wave number, one can get more tightened base of the cone as we have seen. This will definitely helpful in finding finer directionality. However, the amplitude of the cone decreases. This can be easily seen when we take a close look at equation (11). The increase of the wave number yields the decrease in the functional value due to the presence of the negative sign in the exponent. It means that merely increasing the wave number does not always improve the ability to detect the directionality in the signals.

3.2　Cauchy Wavelet

Cauchy wavelet is an alternative tool to the Morlet wavelet in terms of directional selectivity. A very readable reference about Cauchy wavelet was published by [5]. Most of the notations presented below are adopted from that reference. Let $C \equiv C(\alpha, \beta)$ be the convex cone confined by the two unit vectors $\vec{e}_\alpha$, $\vec{e}_\beta$, where $\alpha < \beta$, $\beta - \alpha < \pi$. The axis of the cone is $\vec{\zeta}_{\alpha\beta} = \vec{e}_{(\alpha+\beta)/2}$.

The convex cone can be further defined by

$$
\begin{aligned}
C(\alpha, \beta) &= \left\{ \mathbf{k} \in R^2 : \alpha \leq \arg(\mathbf{k}) \leq \beta \right\} \\
&= \left\{ \mathbf{k} \in R^2 : \mathbf{k} \cdot \boldsymbol{\zeta}_{\alpha\beta} \geq \mathbf{e}_\alpha \cdot \boldsymbol{\zeta}_{\alpha\beta} = \mathbf{e}_\beta \cdot \boldsymbol{\zeta}_{\alpha\beta} > 0 \right\}
\end{aligned}
\tag{12}
$$

where $\mathbf{k}$ represents the wave number vector. We need to introduce the convex dual cone as follows

$$
\tilde{C} \equiv C(\tilde{\alpha}, \tilde{\beta}) = \{ \vec{k} \in R^2, \vec{k} \cdot \vec{k}' > 0, \forall \vec{k}' \in C(\alpha, \beta) \},
\tag{13}
$$

7

where $\tilde{\beta} = \alpha + \pi / 2$, $\tilde{\alpha} = \beta - \pi / 2$. It can be deduced $\vec{e}_{\tilde{\alpha}} \cdot \vec{e}_{\alpha} = \vec{e}_{\tilde{\beta}} \cdot \vec{e}_{\beta} = \sin(\beta - \alpha)$.

The fact that performing the transformation in the Fourier transform is very convenient was mentioned previously. For any $\vec{\eta} \in \tilde{C}$, the Fourier transform of the Cauchy wavelet can be written

$$\hat{\psi}_{lm}^{\{C,\vec{\eta}\}}(\vec{k}) = \begin{cases} (\vec{k} \cdot \vec{e}_{\tilde{\alpha}})^l (\vec{k} \cdot \vec{e}_{\tilde{\beta}})^m e^{-\vec{k} \cdot \tilde{\eta}}, & \vec{k} \in C(\alpha, \beta) \\ 0, & otherwise \end{cases}. \tag{14}$$

With these notations in mind, the mathematical form of the Cauchy wavelet can be written as

$$\psi_{im}^{(C,\vec{\eta})}(\vec{x}) = \frac{i^{l+m+2}}{2\pi} l!m! \frac{\left[\sin(\beta - \alpha)\right]^{l+m+1}}{\left[(\vec{x} + i\vec{\eta}) \cdot \vec{e}_{\alpha}\right]^{l+1} \left[(\vec{x} + i\vec{\eta}) \cdot \vec{e}_{\beta}\right]^{m+1}}, \tag{15}$$

where $l, m \in N$, N represents the integer. If $l = m$, the convex cone is symmetric with respect to the axis of the cone. Then the equation (15) can be written as

$$\psi_{mm}^{(C,\vec{\eta})}(\vec{x}) = \frac{(-1)^{m+1}}{2\pi} (m!)^2 \frac{\left[\sin(\beta - \alpha)\right]^{2m+1}}{\left[(\vec{x} + i\vec{\eta}) \cdot \sigma(\alpha, \beta)(\vec{x} + i\vec{\eta})\right]^{m+1}}, \tag{16}$$

where

$$\sigma(\alpha, \beta) = \begin{pmatrix} \cos\alpha\cos\beta & \sin(\alpha + \beta) \\ \sin(\alpha + \beta) & \sin\alpha\sin\beta \end{pmatrix}. \tag{17}$$

Let's examine the functional shape by taking some numerical values for these parameters. For $C_1 = C(0, \pi / 2)$, $\vec{\eta} = \vec{e}_{\pi/4} = (1,1)$, and $l = m = 1$, the equation (16) becomes

$$\psi_{11}^{(C_1)}(\vec{x}) = \frac{1}{2\pi} \frac{1}{(x+i)^2} \frac{1}{(y+i)^2}. \tag{18}$$

This is a very simplified form of the equation. However, this explains us the reason why this wavelet is called Cauchy wavelet, since each term is the derivatives of the Cauchy kernel $(z+i)^{-1}$. Figure 8 shows the functional shape of the wavelet. It is directed 45° as one can imagine. Let's take $l = m = 4$. The equation for these parameters becomes
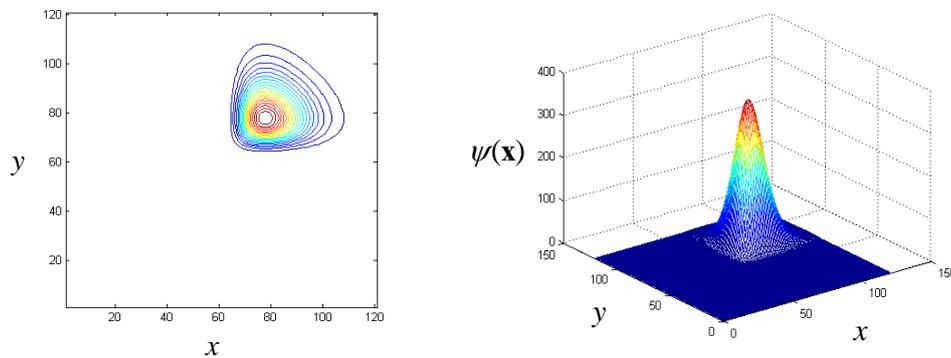
$$\psi_{44}^{(C_1)}(\vec{x}) = \frac{(-1)^5}{2\pi} (4!)^2 \frac{1}{(x+i)^5} \frac{1}{(y+i)^5} \tag{19}$$

The functional shape is shown in figure 9. When we compare the figures 8 and 9, we can notice that the larger the values of l and m, the faster the functional values increases.

To see the asymmetric case of the wavelet, let's take $l = 2$, and $m = 4$. We can see the asymmetric shape of the functional form in figure 10. For $\alpha = -10°$, $\beta = 10°$, the functional shape is presented in figure 11. Now the convex cone can have more directional selectivity due to its narrow area of the cone.

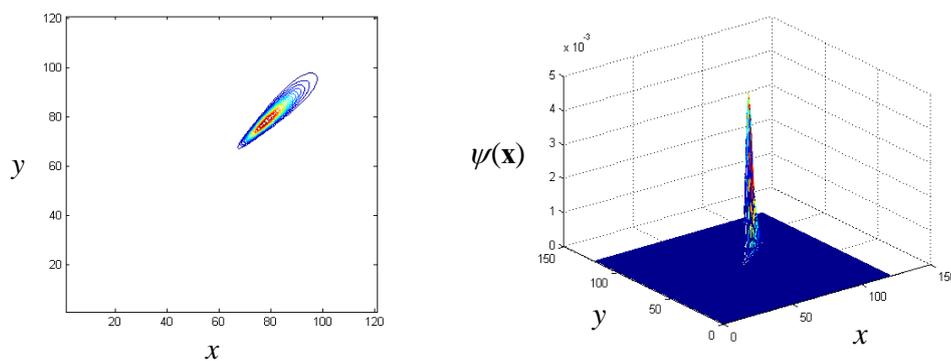Remote Sensing of Wave Directionality
by Two-dimensional Directional Wavelets : Part 1.

Young Jun Yang, Sun Hong Kwon
Seung Geun Park, Jun Soo Park
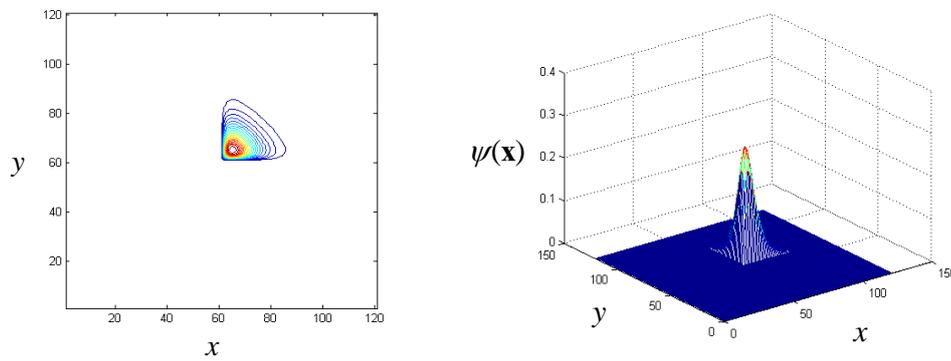
Fig. 8 The functional shape of the Cauchy wavelet: $\alpha = 0°, \beta = 90°, \theta = 45°, l = 1, m = 1$

**Fig. 9** The functional shape of the Cauchy wavelet: $\alpha = 0°, \beta = 90°, \theta = 45°, l = 4, m = 4$
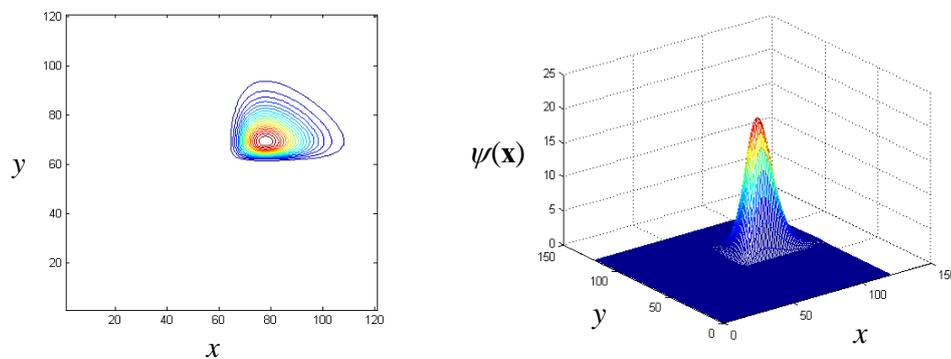
Fig. 10 The functional shape of the Cauchy wavelet: $\alpha = 0°, \beta = 90°, \theta = 45°, l = 2, m = 4$

Fig. 11 The functional shape of the Cauchy wavelet: $\alpha = -10°, \beta = 10°, \theta = 0°, l = 4, m = 4$.

4. Comparison of the two directional wavelets

Let's examine the efficiency of these wavelets on very simple numerical signals. The first signal to be analyzed is shown in figure 12(a). The width of this simple signal was chosen far smaller than the length of the convex cone of the wavelets. The results computed by the Morlet wavelet and Cauchy wavelet are shown in figures 12(b), and 12(c), respectively. The results are presented in polar form of $a^{-1}\left|S(a,\theta,\mathbf{0})\right|$ in coordinates $(k_0 a^{-1}, \theta + \pi/2)$. The $\pi/2$ is added to represent the incident angle of the propagating wave while the signals are inclined to $0°$. As one can imagine that the peaks of the results of the transformation occur at 90° and 270°. We used $\left|\alpha\right| = \beta = 10°$ for an angular envelope which was recommended by [5]. Thus, when it comes to the Cauchy wavelet in this study, $\left|\alpha\right| = \beta = 10°$, and $l = m = 4$ were used. We need to set a threshold to highlight the main contribution. There were no thresholds were applied in the results shown in figures 12(b) and 12(c). The threshold values of 20%, and 30% applied were shown in figures 12(d) and 12(e). The results of 30% threshold will be presented hereafter.

The next signal to be considered is the same as the previous one except the width of the signal which is shown in figure 13(a). The width of the convex cone is smaller than the width of the signal in here. We can imagine that the efficiency of the detection of the signal will be much reduced. The results shown in figures 13(b) and 13(c) confirm this fact. The third example is the case when the signal is tilted as shown in figure 14(a). The results are shown in figures 14(b) and 14(c). The peaks in here are located at 135° and 315° as expected. The next image to be analyzed is presented in figure 15(a). This is equivalent to the case when the two waves are propagating with 90° phase shift. The results are shown in figures 15(b) and 15(c). The next test was done on the discrete images as shown in figure 16(a) which corresponds to the images of short crested waves. Figures 16(b) and 16(c) show the results. The two directional discrete image as shown in figure 17(a) was tested. The results are presented in figures 17(b) and 17(c). This test showed that the directional wavelets can detect multi-directionality in images.
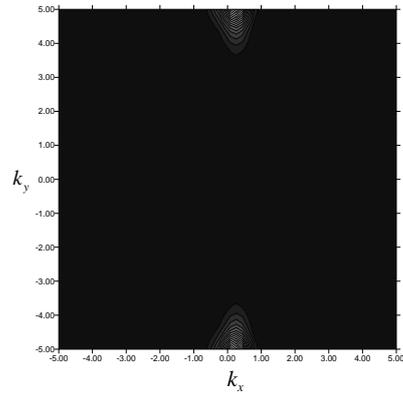
The application of the Morlet wavelet and Cauchy wavelet to more complicated numerical images, and images taken in a wave flume, a river, and an ocean will be presented in part 2 of this paper.
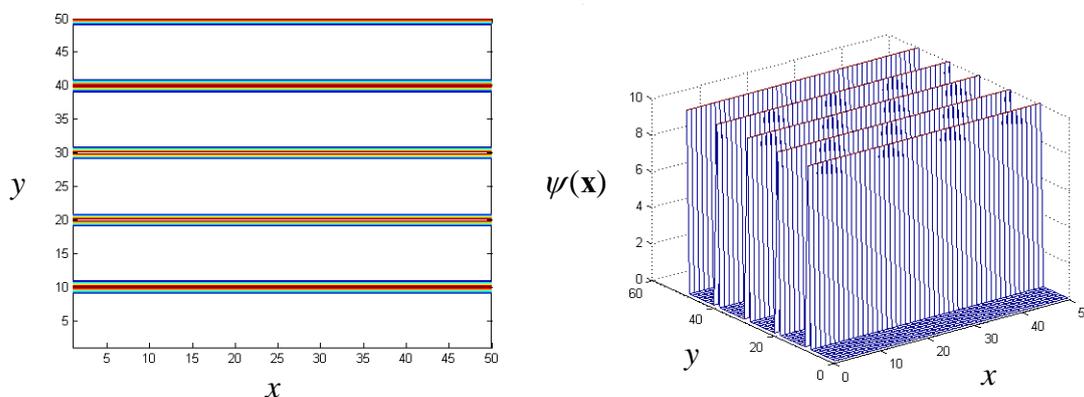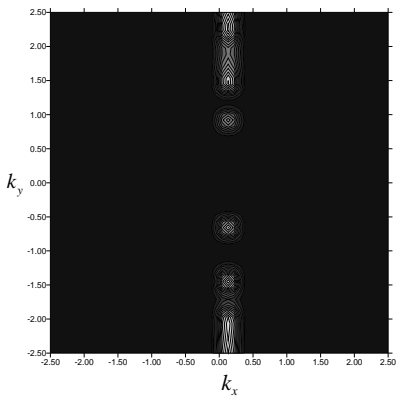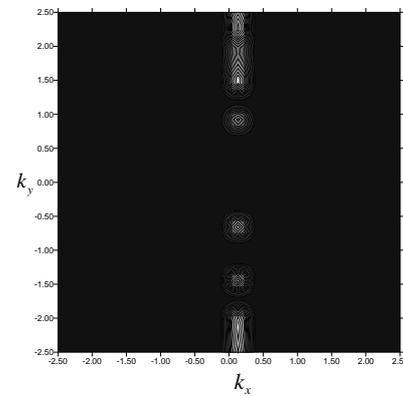

(a) Numerical signal
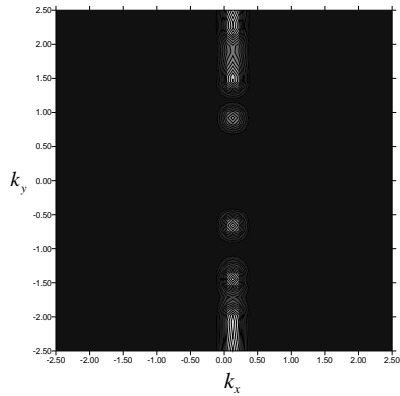
(b) Morlet wavelet transform of Fig. 12(a)
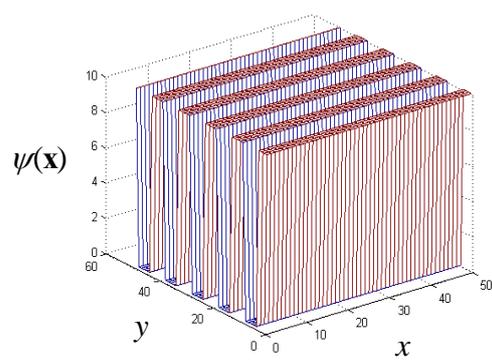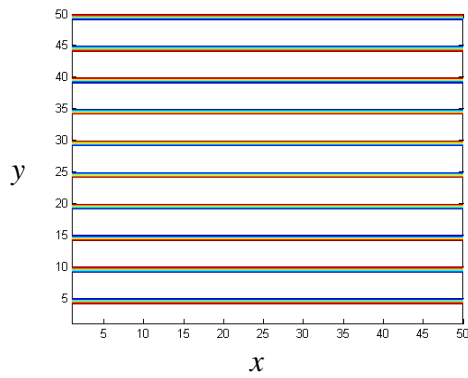

(c). Cauchy wavelet transform of Fig. 12(a)
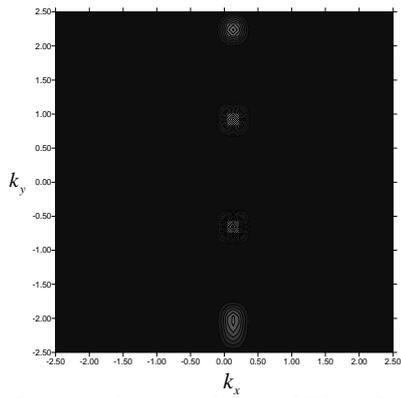

(d) 20% threshold of transformed result
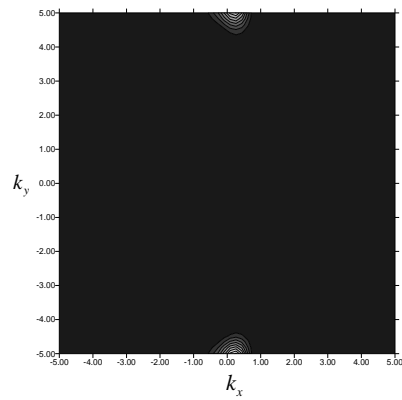

(e) 30% threshold of transformed result

Fig. 12 Comparison result of Morlet wavelet and Cauchy wavelet transform
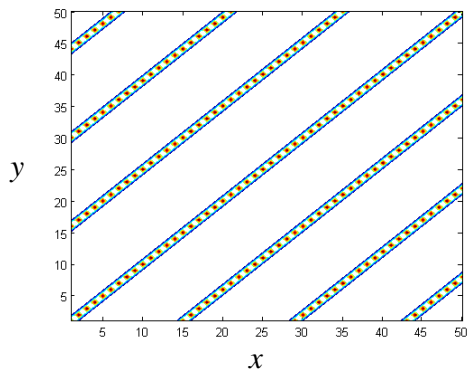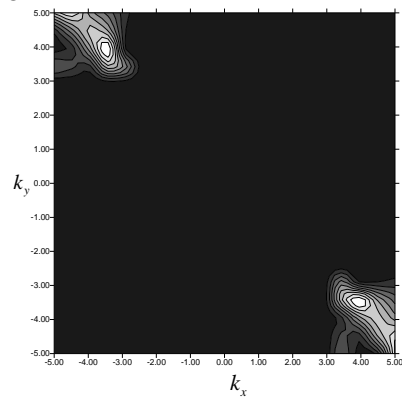

(a) Numerical signal

Young Jun Yang, Sun Hong Kwon,
Seung Geun Park, Jun Soo Park

Remote Sensing of Wave Directionality
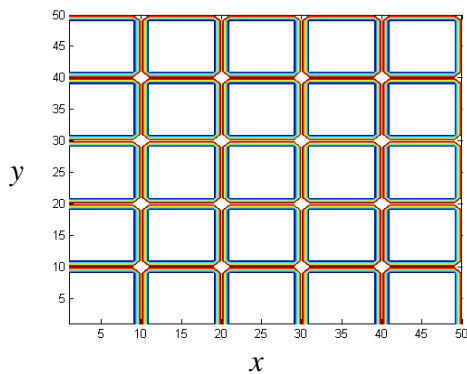by Two-dimensional Directional Wavelets : Part 1.

(b) Morlet wavelet transform of Fig. 13(a)

(c) Cauchy wavelet transform of Fig. 13(a)

Fig. 13 Comparison result of Morlet wavelet and Cauchy wavelet transform
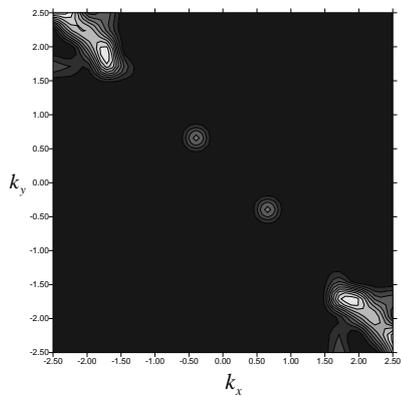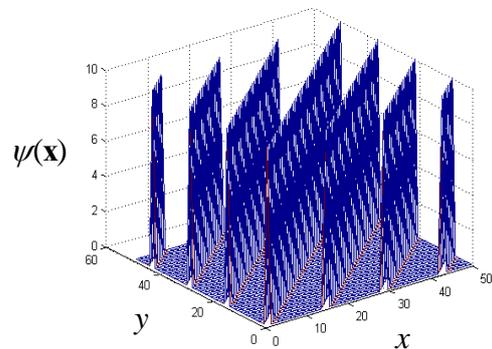
(a) Numerical signal
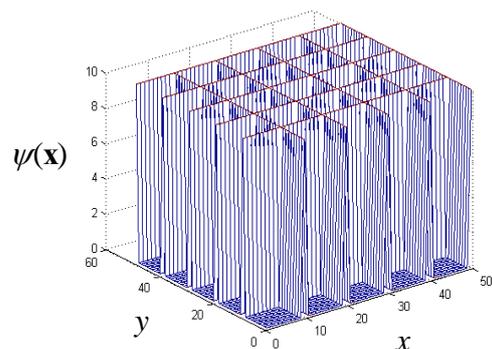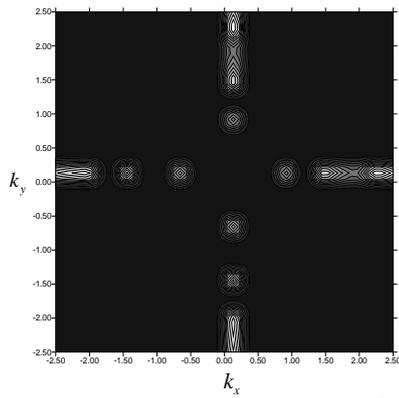

(b) Morlet wavelet transform of Fig. 14(a)

(c) Cauchy wavelet transform of Fig. 14(a)

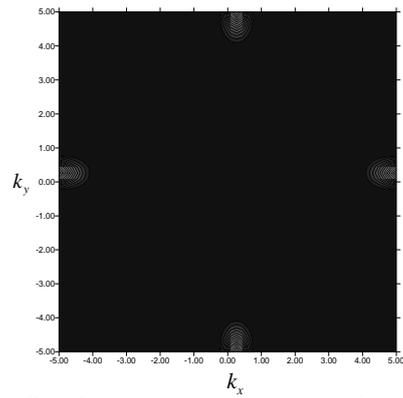**Fig. 14** Comparison result of Morlet wavelet and Cauchy wavelet transform
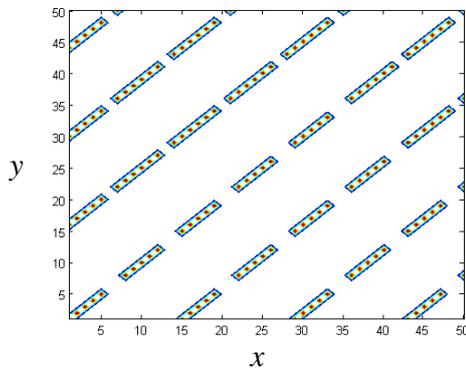

(a) Numerical signal

Remote Sensing of Wave Directionality
by Two-dimensional Directional Wavelets : Part 1.

Young Jun Yang, Sun Hong Kwon
Seung Geun Park, Jun Soo Park
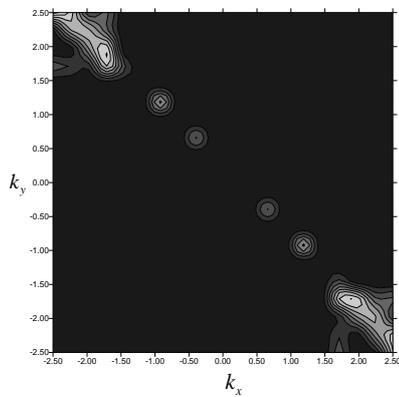

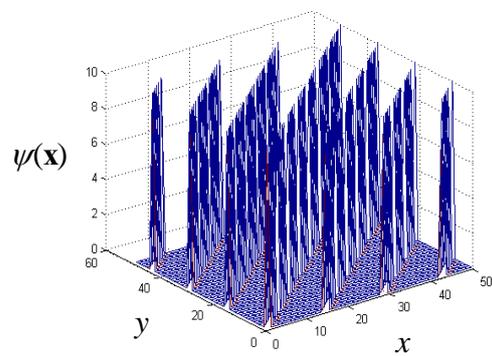(b) Morlet wavelet transform of Fig. 15(a)

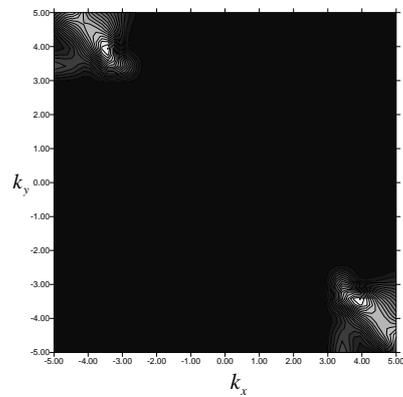(c) Cauchy wavelet transform of Fig. 15(a)

Fig. 15 Comparison result of Morlet wavelet and Cauchy wavelet transform

(a) Numerical signal

(b) Morlet wavelet transform of Fig. 16(a)

(c) Cauchy wavelet transform of Fig. 16(a)

Fig. 16 Comparison result of Morlet wavelet and Cauchy wavelet transform

(a) Numerical signal

13

Young Jun Yang, Sun Hong Kwon,
Seung Geun Park, Jun Soo Park

Remote Sensing of Wave Directionality
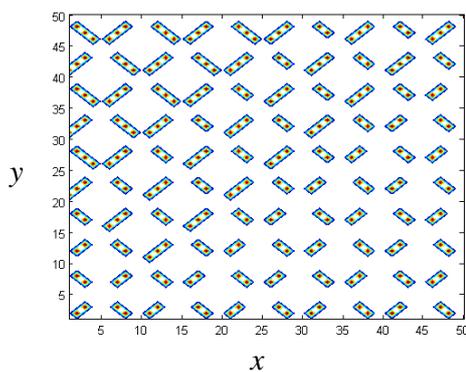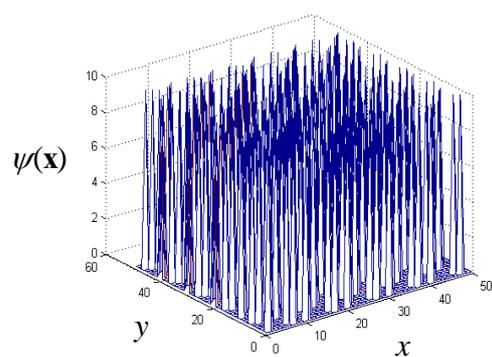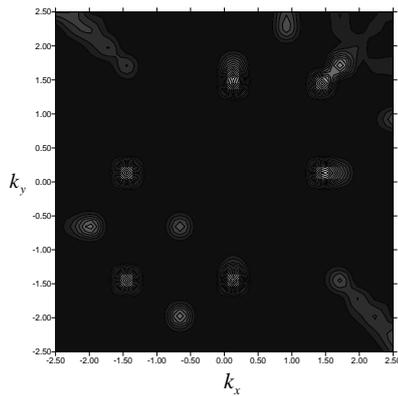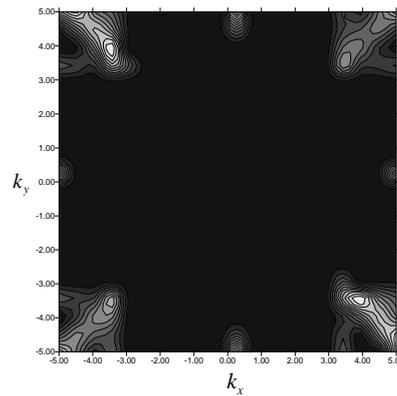by Two-dimensional Directional Wavelets : Part 1.

(b) Morlet wavelet transform of Fig. 17(a)   (c) Cauchy wavelet transform of Fig. 17(a)

Fig. 17 Comparison result of Morlet wavelet and Cauchy wavelet transform

5. Conclusions

The characteristics of directional wavelets were examined. Directional wavelet can be constructed by introducing rotation to directional wavelet. The Morlet and Cauchy wavelet were introduced as a directional wavelet. These wavelets were tested on relatively simple numerical data. It was shown that Morlet and Cauchy wavelet have excellent directional selectivity when the related parameters are chosen appropriately. Once those parameters are chosen, the remaining processes of detection of wave direction are straight forward. The application of Morlet and Cauchy wavelet to the complicated numerical simulations and video images taken in a wave flume, a river, and an ocean will be presented in the part 2 of this paper.

ACKNOWLEDGEMENT

Remote Sensing of Wave Directionality
by Two-dimensional Directional Wavelets : Part 1.

Young Jun Yang, Sun Hong Kwon
Seung Geun Park, Jun Soo Park

REFERENCES

[1]   Paulling, J.R.: Ship's capsizing in heavy seas- The Correlation of theory and experiments, proceedings of international conference on stability of ships and ocean vehicles, University of Strathclyde, Glasgow, 1975.

[2]   Renilson, M.R.: The broaching of ships in following seas', Ph. D thesis, University of Galsgow, 1981.

[3]   Antoine, J.P., Murenzi, R.: Two-dimensional directional wavelets and the scale-angle representation, Signal Processing Vol.52, 1996, pp. 259-281.

[4]   Antoine, J.P., Murenzi, R., Vandergheynst, P.: Directional wavelets revisited: Cauchy wavelets and symmetry detection in patterns, Applied and computational harmonic analysis Vol.6, 1999, pp.314-345.

[5]   Antoine, J.P., Murenzi, R.: The continuous wavelet transform, form 1 to 3 dimensions, in: AKANSU, A. N., SMITH, M. J. T., eds., Subband and wavelet transforms Design and applications, 1996, pp.149-187.

[6]   Wisnoe, W., Gajan, P., Strzelecki, A., Lempereur, C., Mathe, J.M.: The use of the two-dimensional wavelet transform in flow visualization processing, Meyer, Y. and Roques, S., eds, Progress in wavelet analysis and applications, 1993, pp.455-458.

[7]   Rao, A.R., Schunck, B.G.: Computing oriented texture fields, CVGIP: Graphical Models and Image Processing Vol.53, 1991, pp.157-185.

[8]   Watson, A. B., Ahumada, A., J.: A hexagonal orthogonal oriented pyramid as a model of image representation in visual cortex, IEEE transactions of biomedical engineering Vol.37, 1989, pp.97-105.

[9]   Meyer, Y., ed.: Wavelets and their Applications (Proc. Marseille 1989), Springer, Berlin and Masson, Paris, 1991.

[10]   Grossman, A.: Wavelet transform and edge detection, in: Ph. Blanchard, L. Streit, M. Hazewinkel, eds. Stochastic Processes in Physics and Engineering Reidel, Dordrecht, 1985.

[11]   Mallat, S.G.: A theory for multiresolution signal decomposition: The wavelet representation, IEEE Trans. Parrern Anal. Mach. Intell. Vol.11, 1989, pp.674-693.

Young Jun Yang, Sun Hong Kwon
Pusan National University, Dpt. of Naval Architecture and Ocean Engineering, Jangjeon-dong, Geumjeong-gu, Busan, 609-735, Republic of Korea, ybihong@pusan.ac.kr, shkwon@pusan.ac.kr
Seung Geun Park
Global Core Research Center for Ships and Offshore Plants, Pusan National University, Jangjeon-dong, Geumjeong-gu, Busan, 609-735, Republic of Korea
Jun Soo Park
Kyungnam University, Dpt. of Naval Architecture, Ocean and IT Engineering, 7 Kyungnamdaehak-ro, Masanhappo-gu, Changwon-si, Gyeongsangnam-do, Republic of Korea.